

Interaction of polyols with ruthenium metal surfaces in aqueous solution

Lars Peereboom,^a James E. Jackson^b and Dennis J. Miller^{*a}

Received 27th May 2009, Accepted 25th August 2009

First published as an Advance Article on the web 16th September 2009

DOI: 10.1039/b917547b

The irreversible adsorption and decomposition of glycerol and other polyhydric alcohols over ruthenium metal at 298–353 K has been examined in a recirculating microreactor system. The quantity of glycerol (GO), propylene glycol (1,2-propanediol, herein PG), ethylene glycol (EG), or 1,3-propanediol (1,3-PDO) adsorbed on a reduced and evacuated bulk Ru metal powder at saturation is $0.8 \pm 0.2 \mu\text{mol/g}$, a value approximately one-tenth that of CO adsorbed ($9.0 \mu\text{mol/g}$) on the same material. The quantity of polyol adsorbed is independent of temperature, but is strongly affected by the condition of the Ru surface—saturating the metal surface with hydrogen prior to exposure to the polyol significantly reduces the quantity of polyol adsorbed. When they are present together in solution, GO adsorbs more readily than PG, to the point of excluding PG from adsorbing when excess GO is present. Removal of adsorbed species in their original form by heating or flushing with water is not possible, but all carbon is accounted for as desorbed methane when the Ru catalyst is heated under hydrogen.

1. Introduction

The availability of glycerol (GO) as a feedstock for chemicals production has increased dramatically in the past several years, as the formation of biodiesel *via* triglyceride transesterification yields approximately 0.1 kg GO per liter of fuel. This increased supply of low-cost GO has led to announcement of several new commercial processes, including production of epichlorohydrin and propylene glycol (PG).¹ Ironically, epichlorohydrin is to be made *via* the reverse chemical pathway from which GO was previously made commercially. Production of PG from GO, the reaction of interest here, involves metal catalysis in a set of pathways similar to those of other sugar polyols, wherein selectivity to desired products is the primary challenge.

Hydrogenolysis of GO to PG has been examined extensively in the patent and open literature,^{2–7} with the objective of obtaining efficient conversion to PG *via* optimization of catalyst metal and support composition, reaction conditions, and reactor configuration. In some cases, PG yields exceeding 90% have been reported, notably by Dasari *et al.*⁸ and Werpy *et al.*⁹ Dasari *et al.*⁸ have developed a two-step process in which anhydrous GO is initially converted at reduced pressure to acetol (1-hydroxy-2-propanone), which is then readily hydrogenated to PG. Werpy *et al.*⁹ have developed a mixed-metal Co-Ni catalyst to directly convert aqueous GO to PG in a trickle-bed reactor.

This success in converting GO to PG has come with relatively little insight into the mechanistic aspects of the hydrogenolysis chemistry. Lahr and Shanks¹⁰ investigated adsorption and

degradation of PG and ethylene glycol (EG) over a Ru/C catalyst, and found that EG degrades substantially more rapidly than PG. Maris *et al.*¹¹ and Kovacs *et al.*¹² describe a mechanism for GO hydrogenolysis in which the initial step in the reaction is dehydrogenation of GO on the metal surface to form a bound glyceraldehyde analog. Base-catalyzed dehydration leads to 2-hydroxyacrolein, from which tautomerization gives pyruvaldehyde; hydrogenation of either of these intermediates over the metal catalyst leads to PG. The main side reactions of glyceraldehyde include fragmentation *via* retro-Aldol cleavage and hydrogenation of the resulting hydroxyacetaldehyde to form EG, and base-catalyzed rearrangement and deprotonation of hydrated pyruvaldehyde to form lactate. These pathways, long proposed, have been confirmed by the isotopic labeling and intermediate studies of Kovacs *et al.*¹² At high concentrations, aldol condensation chemistry can also form a complex mix of higher molecular weight products.

The adsorption of small molecules onto catalyst surfaces has been previously examined in detail from the gas phase under vacuum conditions using a variety of spectroscopic methods, but to a much more limited extent in the liquid phase. Among promising techniques for liquid phase surface analysis are attenuated total internal reflection infrared spectroscopy (ATR-IR),^{13–20} surface-enhanced Raman scattering (SERS),^{21–25} and electrochemical techniques such as those invoked by Wang *et al.*,²⁶ who used cyclic voltammetry to oxidize and reduce Ru (001) surface while simultaneously measuring X-ray reflectance. They propose that water is chemisorbed on the metal, possibly as a hydroxide.

To investigate the interaction of GO and reaction products with the catalyst metal and thus gain insight into GO hydrogenolysis, we have developed and describe here a solution concentration-based method to measure the extent of species adsorption onto bulk metal ruthenium catalyst. We have chosen ruthenium as a catalyst material because it is widely used in

^aDepartment of Chemical Engineering and Materials Science, Michigan State University, 2527 Engineering Building, East Lansing, Michigan 48824. E-mail: millerd@egr.msu.edu; Fax: (517) 432-1105; Tel: (517) 353-3928

^bDepartment of Chemistry, Michigan State University, East Lansing, Michigan 48824

aqueous phase reactions and because it is readily available in bulk form. We believe this method is the first to measure the quantity of substrate adsorption from the aqueous phase onto an active metal catalyst, and therefore offers an opportunity to better characterize heterogeneous catalytic reactions in water. The GO hydrogenolysis reaction is representative of aqueous-phase reductions that typify biorefinery chemicals production, and thus the method presented is applicable to this class of reactions.

2. Materials and methods

2.1 Materials

Reagent grade glycerol (99%), ethylene glycol (99%), propylene glycol (99%), and 1,3-propanediol (80%) were obtained and used as received from Aldrich Chemical Company. The primary impurity in 1,3-propanediol is *bis*-3-hydroxypropyl ether ($\text{HO}(\text{CH}_2)_3\text{O}$). Ruthenium metal (-100 mesh, Aldrich) was obtained in the form of a bulk “sponge” with moderate porosity;

full characterization of the sponge is given below. All water used was of HPLC-grade. Ultra high-purity hydrogen (99.999%) and argon (99.999%) were obtained from AGA Gas.

2.2 Recirculating microreactor system

Adsorption of various species on Ru metal surfaces was studied in a recirculating microreactor designed to allow precise measurement of small concentration changes in minimal volumes of dilute solution. The system (Fig. 1) consists of an HPLC pump, a tubular vessel (“reactor”) holding the catalyst, an inline sampling system, a partially filled liquid reservoir to facilitate gas-liquid mass transport and liquid volume measurement, and various tubing and valves. The tubular reactor vessel consists of a 10 mm × 100 mm 316 Stainless Steel tube with 2.0 μm frits at the ends. The vessel is immersed in a recirculating oil bath to control temperature. A machined conical insert (Fig. 2) is placed inside the reactor vessel to facilitate liquid mixing and solids fluidization, thus ensuring the best possible contact of the liquid phase with catalyst particles. Fluidization begins at flow

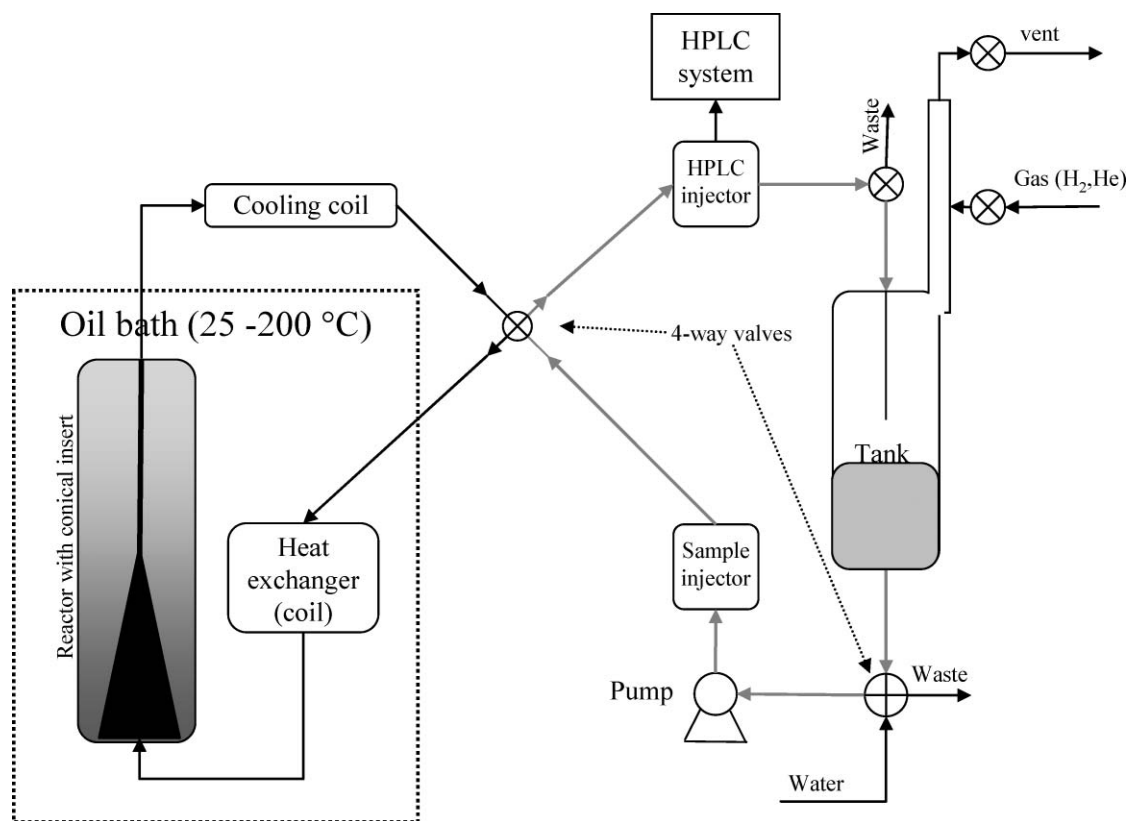


Fig. 1 Recirculating reactor system.

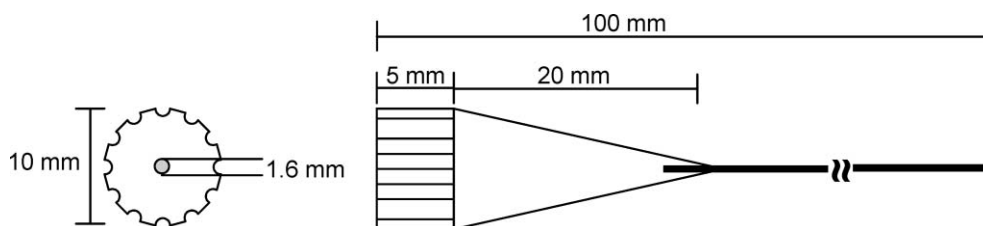


Fig. 2 Stainless steel reactor insert to promote catalyst bed fluidization and liquid-solid contact.

rates above about 2.0 ml/min for the typical Ru particles and liquid solutions used.

Fluid is circulated through the system by a Bio-Rad 1350 HPLC pump with the intake modified with a simple t-fitting to decrease dead volume. The outlet line from the pump goes through a home-made pressure damper consisting of 1.0 m of flattened 0.062" OD SS tubing. The pressure damper prevents excess pressure buildup during valve switching. A set of switching valves either directs fluid through the reactor or through a bypass around the reactor. A 1.0 m coil of 316 stainless steel tubing is placed inside the recirculating bath as a heat exchanger to preheat the liquid entering the reactor. A water cooled heat exchanger is placed after the reactor to protect the system pump and valves from high temperature.

The reservoir, where the system's gas-liquid interface is located, consists of a 12 mm OD \times 100 mm length thick-walled Pyrex tube. The reservoir facilitates dissolution of gases into solution and acts as a sight glass to monitor fluid level in the system. The addition of reservoir gases is controlled by valves and pressure regulation. The addition of substrate into the liquid phase is facilitated by a six port valve that functions as an HPLC sample injector.

The in-line sampling system consists of two Rheodyne 7010 HPLC valves which allow a sample to be withdrawn from the liquid phase for analysis and for the sampling loop to then be flushed with water to prevent mobile phase introduction into the liquid in the reactor system. The HPLC analysis system consists of a Bio-Rad HPX87-H column followed by two detectors, a Perkin-Elmer LC 90 UV detector (210 nm) and a Waters 410 RI detector. The mobile phase is 0.005 M H₂SO₄ and the column is operated isocratically at 40 °C. It should be noted that the HPLC detects and quantifies dissolved gases, distinguishing between He, H₂, Ar, and CH₄, with the response being directly proportional to headspace pressure. Such dissolved gas analysis has not been reported previously (to our knowledge) and is valuable for characterizing aqueous phase reactions.

2.3 Operating procedure

For most experiments, 10 g of Ru sponge was placed in the reactor vessel; the same Ru sponge was used in multiple experiments and was found to exhibit consistent behavior over time. The recirculating system was flushed at 3 ml/min with an argon gas purge and then with degassed HPLC-grade water for at least 10 minutes. The system was then charged with ~12 ml of degassed HPLC-grade water, configured for recirculating mode, placed under 250 psi H₂, and heated to 200 °C for 2–4 h to clean and reduce the catalyst metal surface. During this time, the headspace was exchanged with fresh hydrogen at least three times to remove any gases such as methane formed during reduction. The reactor was then either cooled to 25 °C while recirculating with H₂-saturated water to generate the "H₂-saturated" Ru surface, or was flushed at 200 °C with the argon purge and degassed water for at least one hour, followed by cooling to 25 °C under the same flow, to generate the "H₂-free" Ru surface.

Following the above catalyst preparation, flow was switched to bypass the reactor vessel, the fluid level in the system was adjusted to approximately 13 ml total volume (monitored *via* the

reservoir), a sample of the fluid was taken, and the substrate(s) of interest was(were) introduced. After 30 min, a second sample was taken and flow was directed through the reactor vessel. The liquid phase was then sampled automatically every 30 min until the experiment was completed (typically 12–30 h). Signals from the UV and RI detectors were collected for each sample and stored for analysis. The level in the sight glass and the headspace pressure were recorded at several times during the experiment to monitor leakage and evaporation of the liquid.

2.4 Data analysis

Experimental data collected over the 15 to 30 h adsorption runs consisted primarily of solution concentration *vs.* time. From this raw data, the quantity adsorbed on Ru sponge (mol/g Ru) at any time was determined as the initial quantity (mol) injected into the solution volume, minus the quantity (mol) remaining in solution at that time, minus the quantity (mol) lost in sampling and in leaks from the system, and minus the quantity of substrate consumed in forming product species during the adsorption. The quantity of fluid lost to sampling and leakage was determined *via* the gradations on the liquid reservoir in the recirculating loop. Solution concentration, sampled quantity, and total liquid volume in the system were recorded in an Excel spreadsheet at each sampling time interval and then used to calculate quantity adsorbed on a catalyst mass and surface area basis.

2.5 Characterization of Ru Sponge

The bulk Ru sponge catalyst was characterized by physical and chemical adsorption of gases in a Micromeritics 2010 ASAP instrument. The catalyst was prepared by heating to 623 K for two hours under flowing hydrogen, then evacuating at 623 K for one h, and then cooling under vacuum to 312 K. Gas chemisorption measurements were carried out at 312 K on the prepared surface *via* volumetric dosing to give a total quantity adsorbed. Following this first adsorption, the sample was evacuated at 312 K for 30 minutes, and then a second volumetric adsorption was carried out. The difference between the first and second adsorption was taken to be the quantity of gas chemisorbed. For the Ru sponge, 9.0 ± 1.0 $\mu\text{mol CO/g Ru}$ and 4.5 ± 0.5 $\mu\text{mol H}_2/\text{g Ru}$ were chemisorbed. The observed CO/H₂ ratio of 2.0 is in accordance with literature values^{27,28} reflecting a 1:1 CO:Ru and a 1:1 H:Ru surface stoichiometry for chemisorption. In a separate experiment, a total Ru surface area of 0.5 ± 0.05 m²/g was measured by N₂ adsorption at 78 K in the ASAP 2010 using the BET method of analysis.

3. Results and discussion

Development of the apparatus and method in this study was based upon the expectation that GO and other polyhydric alcohols would adsorb upon exposure to clean Ru metal surfaces and then desorb if flushed with pure water or heated. Somewhat surprisingly, we found that adsorption of any of the species examined onto Ru was irreversible over the temperature range studied (298–353 K). Despite this finding, we observed a clear limit to the quantity of material adsorbed on Ru, indicating that the surface became saturated upon exposure to sufficient substrate and that substrate turnover rate to desorbed products

on the catalyst was low. Further, the carbon contained in the adsorbed species was reliably recovered as desorbed methane gas when the Ru metal was heated in the presence of molecular hydrogen. The adsorption thus appears to be dissociative in nature, likely involves multiple contacts of each molecule with surface Ru atoms, and ultimately involves C-C and C-O bond cleavage. Use of the term “adsorption” is therefore perhaps not entirely appropriate, as adsorption usually implies that the original molecule can be recovered *via* desorption under some conditions. Nevertheless, we use the term adsorption here to represent the interactions of GO and other species with the Ru surface, with the understanding that recovery of the intact adsorbing species was not observed under any conditions despite substantial effort to induce it.

Several control experiments were carried out to ensure that the observed decline in species solution concentration was attributable to adsorption on the Ru metal. Most notably, experiments without Ru catalyst, with unreduced Ru catalyst, or with glass beads in the reactor all resulted in a stable, unchanging species concentration in solution. Only upon exposure to reduced Ru sponge did solution concentration decline over time, indicating species interaction with the Ru surface.

3.1 Adsorption of GO on Ru metal

The adsorption of glycerol (GO) onto Ru metal was examined for GO alone in solution and in combination with propylene glycol (PG). The effects of GO concentration, the presence of hydrogen on Ru, and temperature on the quantity of GO adsorbing onto the Ru surface were investigated and are reported in the following sections.

3.1.1 Effect of GO concentration. Fig. 3 shows the quantity of GO adsorbed on H₂-free Ru sponge at 298 K as a function of final GO solution concentration. Most experiments were run for approximately 18 h starting with initial solution concentrations ranging from 0.1 to 4.2 mM. These data include both 10 and 20 g loadings of ruthenium sponge in the reactor with a total liquid volume of 11–13 ml. As seen in Fig. 3, as long as sufficient GO is present, the maximum quantity adsorbed is 0.8 ± 0.2 $\mu\text{mol/g}$ Ru. This quantity is approximately 10% of the quantity of CO (9 $\mu\text{mol CO/g Ru}$) or H (4.5 $\mu\text{mol H}_2/\text{g Ru}$) adsorbed on Ru *via* chemisorption. If a 1:1 CO:Ru adsorption stoichiometry is assumed, GO adsorption onto the metal surface covers

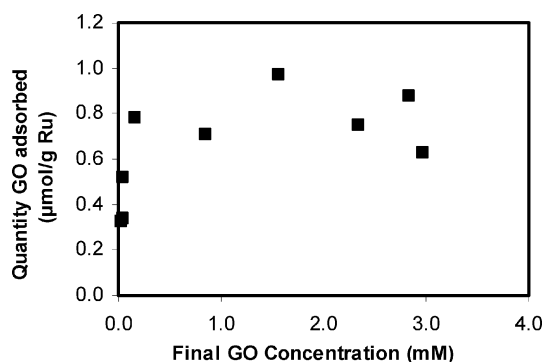


Fig. 3 Quantity of GO adsorbed on H₂-free Ru sponge at 298 K for initial GO concentrations ranging from 0.1 to 4.2 mM.

approximately ten Ru atoms, a number sufficient to provide multiple contact points during the adsorption process.

Similar adsorption behavior was observed in experiments where GO was added stepwise over the course of the experiment. As an example, Fig. 4 gives both solution concentrations and quantities adsorbed *vs.* time for an experiment in which GO is added to a hydrogen-free Ru surface in two aliquots (at $t = 0$ and $t = 16$ h), the first giving a solution concentration of 0.4 mM and the second 0.8 mM. The first aliquot was entirely adsorbed, and the second led to saturation of the surface. Fig. 4 also shows the formation of ethylene glycol (EG) and propylene glycol (PG) as GO hydrogenolysis products at 298 K, indicating that chemical pathways are accessible at this low temperature, albeit with limited activity (2–4% GO conversion over 40 h of exposure). Fig. 4 also gives an indication of the kinetics of adsorption: following a very rapid initial drop, the first order rate constant for GO adsorption from solution is ~ 0.2 h⁻¹.

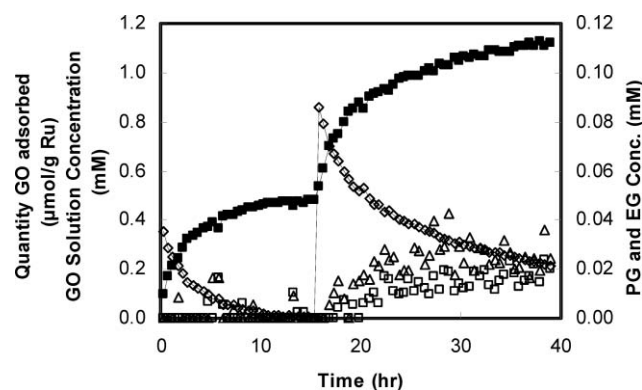


Fig. 4 Adsorption of GO on H₂-free Ru sponge with GO addition (0.8 mM) at $t = 0$ and $t = 16$ h. Conditions: 12 ml fluid, 10 g Ru sponge, 298 K. Both quantity adsorbed ($\mu\text{mol/g}$) and GO solution concentration (mM) are plotted on left axis. EG and PG concentrations (mM) are plotted at 10 \times on right axis. (\diamond) – GO solution concentration; (\blacksquare) – GO adsorbed; (\square) – PG solution concentration; (\triangle) – EG solution concentration.

3.1.2 Effect of hydrogen. Adsorption of GO on “H₂-saturated” and “H₂-free” Ru surfaces (described above) at 298 K is reported in Table 1 for two different initial concentrations of GO. Saturating the Ru surface with hydrogen prior to exposure to GO significantly reduces the quantity of GO that adsorbs. This finding is in accord with prior mechanistic analysis of GO hydrogenolysis, in which it has been postulated¹² that the first step is adsorption of GO onto the metal surface *via* dehydrogenation to form an aldehyde analog. The driving force for this first step is the ability of the metal to cleave C-H and/or C-O bonds in GO and accept the hydrogen atoms from GO onto its surface. At the high temperatures (>150 °C) where hydrogenolysis occurs readily, the metal can continuously catalyze hydrogenolysis because hydrogen preferably desorbs from the surface and thus active sites are available for reaction.²⁹ At the low temperatures (<80 °C) used in this work, however, hydrogen is stably adsorbed onto Ru and thus can saturate the surface.²⁹ Presaturation of Ru with hydrogen thus limits GO dehydrogenation, because the hydrogen-saturated metal surface

Table 1 Adsorption of polyols from aqueous solution onto ruthenium sponge (298 K, 24 h adsorption)

Species	State of Ru surface	Initial solution concentration (mM)	Final solution concentration (mM)	Quantity adsorbed ($\mu\text{mol/g Ru}$)
GO	H ₂ -free	0.4	-0	0.32 ± 0.08
GO	H ₂ -free	4.2	2.4	0.75 ± 0.2
GO	H ₂ -saturated	0.4	-0	0.08 ± 0.02
GO	H ₂ -saturated	4.2	3.1	0.30 ± 0.08
PG	H ₂ -free	0.5	-0	0.18 ± 0.04
PG	H ₂ -free	5.4	4.0	0.75 ± 0.2
PG	H ₂ -saturated	6.0	5.2	0.1 ± 0.02
EG	H ₂ -free	7.6	6.2	0.9 ± 0.2
1,3-PDO	H ₂ -free	3.8	1.6	0.85 ± 0.2

is unable to activate C-H or C-O cleavage in GO and accept the hydrogen atoms liberated.

3.1.3 Effect of temperature. Experiments were run at temperatures from 298 to 353 K under otherwise identical conditions (4.0 mM GO, 20 g Ru sponge, and standard metal preparation). Fig. 5 shows that the quantity of GO adsorbed increases only slightly with temperature over the range investigated, although multiple experiments at the same temperature revealed substantial experimental uncertainty ($\pm 0.2 \mu\text{mol/g Ru}$) in the total quantity adsorbed.

Significant decomposition of GO takes place on the Ru surface at higher temperatures, as evidenced by product formation shown in Fig. 6. Fig. 7 describes the overall pathway for GO decomposition and product formation on Ru. As temperature increases, so does the extent of C-C and C-O bond cleavage in the adsorbed glyceraldehyde analog on Ru. At 298 K, surface bound hydrogen atoms produced by the adsorption of GO are stable on Ru, and the adsorbed glyceraldehyde analog is stable, so little methane formation is observed. At 333 K, hydrogen atoms on Ru are still adsorbed²⁹ but less strongly so, and thus

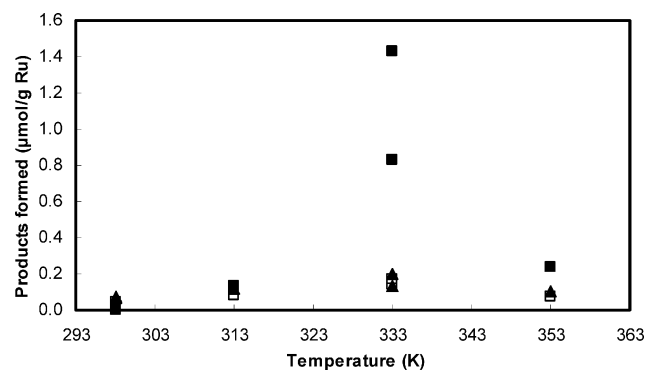


Fig. 6 Decomposition products formed during GO adsorption onto Ru sponge. Conditions: 4.1 mM initial GO concentration, 20 g Ru sponge, 18–20 h adsorption. Multiple experiments are included at 298 K and 333 K. (■) – CH₄; (▲) – EG; (□) – PG.

are capable of forming methane by reaction with the adsorbed carbon-containing fragments of decomposing GO on the Ru surface. At 353 K, hydrogen produced *via* GO adsorption and decomposition desorbs rapidly²⁹ from the Ru surface and exits

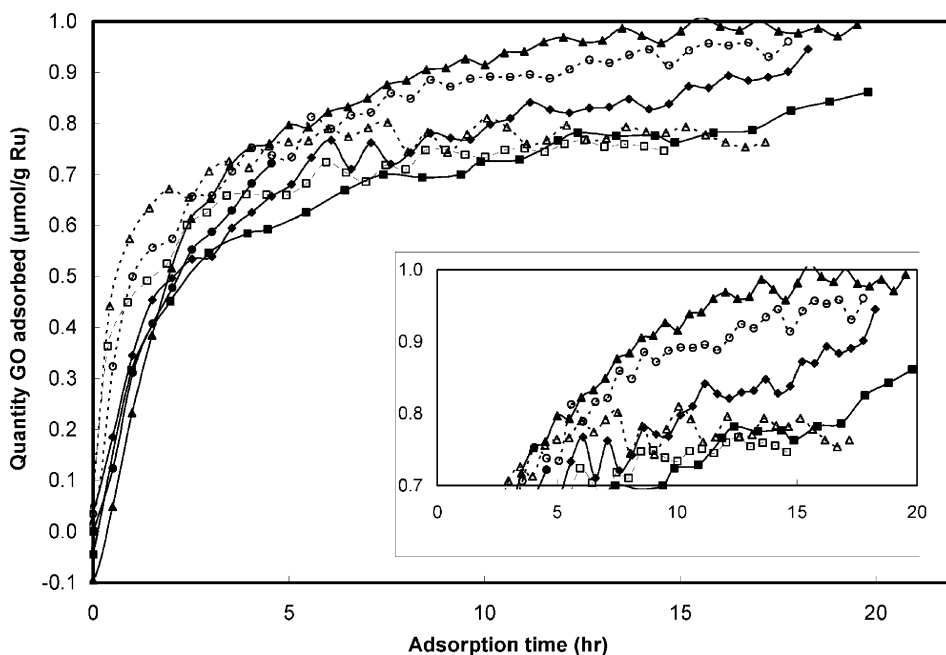


Fig. 5 GO adsorption on H₂-free Ru sponge at several temperatures. Conditions: 4.2 mM initial GO concentration, 20 g Ru sponge. (■, □) – 298 K; (◆) – 313 K; (△, ▲) – 333 K; (○) – 353 K. Duplicate experiments are reported at 298 K and 333 K. Inset shows magnification of upper region of graph.

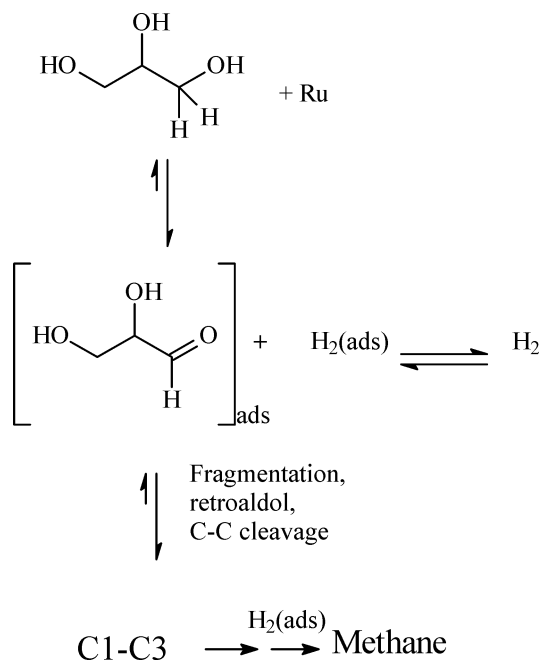


Fig. 7 Adsorption and decomposition of glycerol on ruthenium.

the system *via* the gas phase, leaving GO fragments on the Ru surface without the hydrogen required to convert them to methane. It is noteworthy that the quantity of GO converted to products at 333 K after 18 h is as much as 40% of that adsorbed on the Ru surface. The difference in the quantity of methane formed (0.8 $\mu\text{mol/g}$ vs. 1.4 $\mu\text{mol/g}$, Fig. 6) during the two identical experiments at 333 K reflects uncertainty in experimental results.

Several additional observations regarding hydrogen are noteworthy, given the effect of hydrogen presaturation on the extent of glycerol adsorption (Table 1). First, adding H_2 to the recirculating system at 298 K during GO adsorption immediately halts the adsorption of GO. Second, adding H_2 to the system at 353 K results in both the cessation of GO adsorption and the conversion of the GO carbon adsorbed to methane. Third, adding H_2 to the system and increasing the temperature to 473 K results in the conversion of all carbon from GO, both adsorbed and in solution, to methane.

Details of the structure and extent of interaction of the adsorbed GO species with the Ru surface at low temperatures are as yet uncertain. While there is strong evidence from labeling and reactivity studies^{11,12} that dehydrogenation to form a bound aldehyde analog is the first step in adsorption, it is not certain to what extent additional dehydrogenation of the adsorbed species takes place. However, the quantity of GO adsorbed and our inability to recover adsorbed species intact from the Ru surface suggest that, in many cases, complete decomposition of the adsorbed species takes place. The fact that adsorbed GO occupies an area equivalent to approximately ten Ru atoms on the surface (as related by relative quantities of CO and GO adsorbed) suggests that $-\text{C}-$ and $-\text{O}-$ adsorbed on Ru from dissociated GO cover essentially those ten atoms. The inability to recover adsorbed GO intact from the Ru surface, either by simply heating Ru to 473 K or flushing the system

with fresh water and then heating to 473 K, suggest that the adsorbed GO is no longer intact. We thus surmise that multiple adsorption bonds are formed and C-C and C-O bond cleavage takes place as GO adsorbs and dehydrogenates on the Ru surface.

3.2 Adsorption of PG, EG, and 1,3-PDO

Adsorption of several polyols was carried out at 298 K *via* the same procedure applied for GO adsorption. The results, displayed in Table 1, show adsorption behavior similar to that of GO. Adsorption at low concentration (0.5 mM) corresponds to depletion of the glycol from solution; at high concentrations (3.8–6.0 mM), the quantities adsorbed by all three polyols are $0.8 \pm 0.2 \mu\text{mol/g}$, similar to that of GO. Further, presaturation of the Ru surface with hydrogen leads to a decline in PG adsorption similar to that observed for GO. This finding is consistent with the notion that the mechanism for GO adsorption also applies to PG. For PG, lactic acid is the main desorption product and is only seen in the high concentration run with no H_2 present. Again, this product is consistent with PG dehydrogenation leading to bound lactaldehyde (2-hydroxypropionaldehyde) that is hydrated and further dehydrogenated to lactate in the aqueous environment. The adsorption of 1,3-PDO led to significant quantities of several decomposition products including ethanol, formic acid (FA), acetic acid (AA), and 3-hydroxypropanoic acid (3-HPA). Compared to PG, the larger product slate from 1,3-PDO reflects the fact that activation of 1,3-PDO *via* dehydrogenation opens up an array of decomposition pathways dominated by retro-aldol cleavage to C_2 and C_1 fragments. This finding is consistent with the observation that direct hydrogenolysis of 3-HPA only gives moderate yields of 1,3-PDO relative to those for PG from lactic acid, because 1,3-PDO and/or the implicit 3-hydroxypropanal en route to it decompose rapidly at the catalyst surface as they are formed.

3.3 Binary adsorption of GO and PG

To examine the difference in adsorption properties of GO and PG on Ru, experiments were run at 298 K with 10 g Ru sponge with both species present. In one run, PG was added first followed by GO; in another run, GO adsorption was followed by PG; and in a third run, both were added at the same time.

The quantity of PG adsorbed after 16 hours of circulation was $\sim 0.18 \mu\text{mol/g}$ Ru from 0.5 mM solution (Fig. 8a) and $0.6 \mu\text{mol/g}$ Ru from 5.0 mM solution. At 16 h, 0.4 mM GO was added to the solution and allowed to adsorb for 20 hours (Fig. 8a). For both the low and high PG loadings, 0.1 to 0.2 $\mu\text{mol/g}$ Ru GO adsorbed, but very little additional PG adsorbed when GO was present. The total quantity of combined species adsorbed ($\sim 0.8 \mu\text{mol/g}$) at the completion of experiment for the high PG concentration was the same within uncertainty as that observed for single species adsorption.

When the order of adsorption was reversed, 0.27 μmol GO/g Ru was adsorbed following exposure of the Ru sponge to a 0.5 mM GO solution for 16 h, (Fig. 8b). Addition of PG at 16 h at a concentration of 0.5 mM led to no detectable PG adsorption. A small additional quantity of GO was observed to adsorb following PG addition.

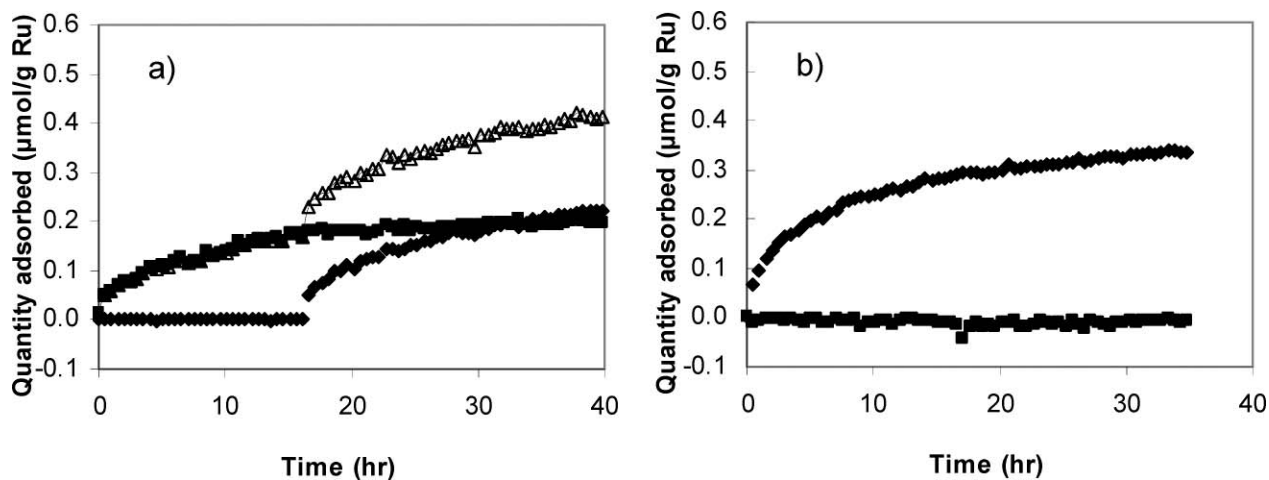


Fig. 8 a) Adsorption of PG (0.5 mM at $t = 0$) followed by GO adsorption (0.4 mM added to solution at $t = 18$ h) on 10 g H_2 -free Ru sponge at 298 K. (- \blacklozenge -) GO; (- \blacksquare -) PG; (- \triangle -) total. b) Adsorption of GO (0.5 mM at $t = 0$) followed by PG adsorption (0.5 mM added to solution at $t = 18$ h) on 10 g H_2 -free Ru sponge at 298 K. (- \blacksquare -) PG; (- \blacklozenge -) GO.

Simultaneously introducing GO and PG into the recirculating reactor at concentrations of 0.5 mM each led to 0.18 $\mu\text{mol GO/g Ru}$ and 0.07 $\mu\text{mol PG/g}$ adsorbed after 16 h. The ratio of adsorbed quantities ($\sim 2.6:1$ GO:PG) is very close to the ratio of initial rates of GO and PG adsorption as estimated by the initial slopes of the adsorption curves ($t = 0$) in Fig. 8.

Results of the GO and PG adsorption experiments are consistent with preferential GO adsorption on the Ru surface. In the sequential experiments, adsorbing GO first entirely eliminates the subsequent adsorption of PG, while GO is still able to adsorb and halts PG adsorption even when it is added after PG. The simultaneous adsorption shows that the two species compete for sites from a kinetic standpoint. This observed preference of GO adsorption may be partially explained by the fact that GO has two terminal sites (C1 and C3), so it should adsorb twice as rapidly as PG which has only a single (C1) terminal site. In all of these binary experiments, the low concentration of GO added (0.5–0.7 mM) led to essentially all GO being adsorbed from solution—further evidence that GO strongly and irreversibly adsorbs on the Ru surface at relatively low temperatures.

4. Conclusions

The adsorption of GO, PG, and other polyhydric alcohols from the aqueous phase onto a reduced, H_2 -free ruthenium metal surface is consistent with earlier evidence¹² that the initial step in polyol hydrogenolysis is dehydrogenation to form a bound aldehyde and adsorbed molecular hydrogen. The maximum quantity adsorbed for all species is approximately 0.8 $\mu\text{mol/g Ru}$ over the temperature range 298–353 K. The adsorbed species do not desorb intact; instead, addition of hydrogen results in all carbon present desorbing as methane. Saturation of the Ru surface with hydrogen prior to adsorption reduces the quantity of polyol adsorbed by as much as 80%. Slow decomposition of the adsorbed species takes place even at room temperature. Competitive adsorption experiments show that GO preferentially adsorbs over PG, the weaker adsorption of PG

perhaps explaining why very little PG degradation is observed in GO hydrogenolysis.

Acknowledgements

The support of the U.S. Department of Agriculture, National Research Initiative under Grant #2003-35504-12879 is gratefully acknowledged. Additional support was provided by the U.S. Department of Energy through Battelle Pacific Northwest National Laboratory.

References

- 1 S. A. Shelley, *Chem. Eng. Progr.*, 2007, **103**, 6.
- 2 M. Pagliaro, R. Ciriminna, H. Kimura, M. Rossi and C. Della Pina, *Angew. Chem., Int. Ed.*, 2007, **46**, 4434.
- 3 J. Feng, M. L. Yuan, H. Chen and X. J. Li, *Progr. Chem.*, 2007, **19**, 651.
- 4 B. Casale and A. M. Gomez, *US Pat.* 5 214 219, 1993.
- 5 L. Schuster and M. Eggersdorfer, *US Pat.* 5 616 817, 1997.
- 6 T. Miyazawa, S. Koso, K. Kunimori and K. Tomishige, *Appl. Catal., A*, 2007, **329**, 30.
- 7 S. Wang and H. Liu, *Catal. Lett.*, 2007, **117**, 62.
- 8 M. A. Dasari, P. Kiatsimkul, W. Sutterlin and G. Suppes, *Appl. Catal., A*, 2005, **281**, 225.
- 9 T. Werpy, J. G. Frye, A. Zacher, D. J. Miller, *US Pat.* 6 841 085 B2, 2005.
- 10 D. Lahr and B. H. Shanks, *Ind. Eng. Chem. Res.*, 2003, **42**, 5467.
- 11 E. Maris and R. Davis, *J. Catal.*, 2007, **249**, 328.
- 12 D. G. Kovacs, J. E. Jackson and D. J. Miller, *Abstracts of Papers of the American Chemical Society*, 2001, **221**, U177.
- 13 N. Bonalumi, A. Vargas, D. Ferri, T. Burgi, T. Mallat and A. Baiker, *J. Am. Chem. Soc.*, 2005, **127**, 8467.
- 14 A. Vargas, D. Ferri and A. Baiker, *J. Catal.*, 2005, **236**, 1.
- 15 B. Keresztesi, D. Ferri, T. Mallat and A. Baiker, *J. Phys. Chem.*, 2005, **109**, 958.
- 16 G. M. Hamminga, G. Mul and J. Moulijn, *Chem. Eng. Sci.*, 2004, **59**, 5479.
- 17 G. Lefevre, *Adv. Colloid Interface Sci.*, 2004, **107**, 109.
- 18 G. Mul, G. Hamminga and J. A. Moulijn, *Vib. Spectrosc.*, 2004, **34**, 109.
- 19 A. R. Hind, S. K. Bhargava and A. McKinnon, *Adv. Colloid Interface Sci.*, 2001, **93**, 91.

-
- 20 B. J. Ninness, D. W. Bousfield and C. P. Tripp, *Appl. Spectrosc.*, 2001, **55**, 655.
- 21 R. M. Lazorenko-Manevich, *Russ. J. Electrochem.*, 2005, **41**, 799.
- 22 Z. Tian and B. Ren, *Annu. Rev. Phys. Chem.*, 2004, **55**, 197.
- 23 A. G. Brolo, D. E. Irish and B. D. Smith, *J. Mol. Struct.*, 1997, **405**, 29.
- 24 M. W. Urban, *J. Adhes. Sci. Technol.*, 1993, **7**, 1.
- 25 A. Otto, *J. Raman Spectrosc.*, 1991, **22**, 743.
- 26 W. X. Wang, N. S. Marinkovic, H. Zajonz, B. M. Ocko and R. R. Adzic, *J. Phys. Chem. B*, 2001, **105**, 2809.
- 27 J. G. Goodwin, *J. Catal.*, 1981, **68**, 227–232.
- 28 T. Narita, H. Miura, K. Sugiyama and T. Matsuda, *J. Catal.*, 1987, **103**, 492–495.
- 29 D. W. Goodman, T. E. Madey, M. Ono and J. T. Yates, *J. Catal.*, 1977, **50**, 279–290.